

# Viscous overstability and eccentricity evolution in three-dimensional gaseous discs

Henrik N. Latter and Gordon I. Ogilvie

*Department of Applied Mathematics and Theoretical Physics, University of Cambridge, Centre for Mathematical Sciences, Wilberforce Road, Cambridge CB3 0WA*

8 May 2018

## ABSTRACT

We investigate the growth or decay rate of the fundamental mode of even symmetry in a viscous accretion disc. This mode occurs in eccentric discs and is known to be potentially overstable. We determine the vertical structure of the disc and its modes, treating radiative energy transport in the diffusion approximation. In the limit of very long radial wavelength, an analytical criterion for viscous overstability is obtained, which involves the effective shear and bulk viscosity, the adiabatic exponent and the opacity law of the disc. This differs from the prediction of a two-dimensional model. On shorter wavelengths (a few times the disc thickness), the criterion for overstability is more difficult to satisfy because of the different vertical structure of the mode. In a low-viscosity disc a third regime of intermediate wavelengths appears, in which the overstability is suppressed as the horizontal velocity perturbations develop significant vertical shear. We suggest that this effect determines the damping rate of eccentricity in protoplanetary discs, for which the long-wavelength analysis is inapplicable and overstability is unlikely to occur on any scale. In thinner accretion discs and in decrection discs around Be stars overstability may occur only on the longest wavelengths, leading to the preferential excitation of global eccentric modes.

**Key words:** accretion, accretion discs — hydrodynamics — instabilities

## 1 INTRODUCTION

Accretion discs may support a wide variety of wave motions. The basic epicyclic tendencies of orbiting particles, which result from gravitational and inertial forces, can combine with acoustic and buoyancy effects to allow many different modes of oscillation. In some cases self-gravitational or magnetic forces may also be significant.

Waves in accretion discs are usually analysed without regard to the shear stress that is necessarily present in order to transport angular momentum and facilitate accretion. This stress, probably of turbulent origin, is most often modelled as deriving from an effective viscosity, which might be expected always to damp the waves. However, Kato (1978) found that ‘pulsational instability’ can occur under certain circumstances, by analogy with the ‘overstability’ of stellar oscillations (Eddington 1926). In particular, if the stress responds to wavelike perturbations in a certain way, a viscous overstability is possible, in which some of the energy being drawn by the stress from the differential rotation of the disc is diverted into waves of growing amplitude. This effect has long been discussed as a means of exciting disturbances in accretion discs and planetary rings (e.g. Kato & Fukue 1980; Borderies, Goldreich & Tremaine 1985;

Papaloizou & Stanley 1986; Kato, Honma & Matsumoto 1988; Papaloizou & Lin 1988; Schmit & Tscharnuter 1999).

The stresses in accretion discs and planetary rings are probably not accurately described as arising from an isotropic viscosity in the sense of the Navier–Stokes equation. Nevertheless, the general principle that overstability may occur as the stress responds to wavelike perturbations applies to all discs, even if the details are difficult to quantify.

Waves in thin discs are often studied in a two-dimensional approximation in which motion in the vertical ( $z$ ) direction, perpendicular to the orbital plane, is absent and the disc remains in vertical hydrostatic balance. This approximation is highly convenient but can only be justified under exceptional circumstances and indeed eliminates almost all of the wave modes. The original analysis of Kato (1978) was in fact based on a three-dimensional disc, but at the time of writing of his paper the behaviour of waves in such discs was not fully understood. Subsequently it was shown that a thin disc acts as a waveguide that conducts in the radial direction a set of discrete modes having distinct vertical structures determined from an eigenvalue problem (Okazaki & Kato 1985; Loska 1986; Lubow & Pringle 1993; Korycansky & Pringle 1995). Some of these can be classi-

fied as f, p and g modes by direct analogy with stellar oscillations (Ogilvie 1998). Generally the propagation of these waves is restricted to certain intervals of radius because they encounter turning points at Lindblad or other resonances.

Perhaps of greatest interest among these is the  $f^e$  mode, the fundamental mode of even symmetry about the midplane, in the classification of Ogilvie (1998). This mode is the closest equivalent of the inertial-acoustic wave (or ‘density wave’) that appears in the analysis of a two-dimensional disc. Its eigenfunction involves horizontal velocity perturbations which are symmetric about the midplane and have no nodes in their vertical structure, but which in general do vary significantly with  $z$  and are accompanied by vertical velocity perturbations. This is by far the dominant mode excited by tidal forcing at Lindblad resonances, and its excitation, propagation and dissipation have been investigated by Lubow & Ogilvie (1998), Ogilvie & Lubow (1999) and Bate et al. (2002). The  $f^e$  mode is also the obvious candidate for viscous overstability. However, Kato (1978) assumed that the horizontal velocities would be independent of  $z$ , which is not true of the  $f^e$  mode. A self-consistent linear calculation of overstable modes in a three-dimensional disc has never been carried out, though the nonlinear behaviour of axisymmetric discs with full vertical structure has been simulated by Kley et al. (1993). They report that when  $\alpha$  is larger than a small value the disc exhibits global, axisymmetric, overstable modes confined to the outer edge of the computational domain.

The question of overstability also arises in the theory of eccentric discs. A small eccentricity can be regarded as a special type of wave motion, corresponding to azimuthal wavenumber  $m = 1$ , propagating in a circular disc. Although the viscous overstability has been discussed mainly for axisymmetric waves, the local dynamics of waves of modest azimuthal mode number in a thin disc is equivalent to that of axisymmetric waves. Studies of eccentric viscous discs in two and three dimensions have indeed found overstability (Lyubarskij, Postnov & Prokhorov 1994; Ogilvie 2001), meaning that the eccentricity often has a negative diffusion coefficient and would grow spontaneously and preferentially on small radial scales (comparable to the disc thickness). This is contrary to the intuitive concept that viscosity should damp eccentricity. It is important to note that  $m = 1$  waves propagating in a (nearly) Keplerian disk are quite exceptional in that they can maintain a long radial wavelength over an extended radial distance.

Understanding the growth or decay rate of eccentricity in a disc is of great importance. For example, in protoplanetary systems, eccentricity is a joint property of the planets and the disc since it is exchanged through secular and resonant interactions. The behaviour of eccentricity within the disc therefore affects the eccentricity of all the planets as well.

The decretion discs around Be stars appear to have global eccentric modes which may be excited by the viscous overstability (Kato 1983; Okazaki 1991). However, since the overstability is believed to grow preferentially on a wavelength comparable to the disc thickness it may be difficult to account for the appearance of coherent global modes.

It was shown by Ogilvie (2001) that the criterion for overstability is different in two- and three-dimensional discs, and that it can be suppressed either by introducing a suf-

ficiently large bulk viscosity or by using a more sophisticated model of the turbulent stress that involves a sufficiently large relaxation time. Latter & Ogilvie (2006) have also shown that the viscous overstability is suppressed in dilute planetary rings when the non-Newtonian nature of the stress is taken into account. The analysis of eccentric discs by Ogilvie (2001) assumes that the eccentricity is independent of  $z$ , which is correct if sufficiently large stresses are present to couple different strata in the disc. In a low-viscosity disc, however, the eccentricity could vary with  $z$  and might be better described by the structure of the  $f^e$  mode.

We are led, therefore, to investigate the behaviour of wave modes in a viscous disc. In Section 2 we analyse a simple two-dimensional model by way of introduction, while the full three-dimensional model is presented in Section 3. We describe the methods of numerical solution in Section 4 and the results follow in Section 5. We conclude with a summary and discussion in Section 6.

## 2 TWO-DIMENSIONAL MODEL

In order to describe disturbances with wavelengths that are short compared to the radial coordinate  $r$  we use the model of the shearing sheet (Goldreich & Lynden-Bell 1965). A point in the disc at reference radius  $r_0$  and orbiting with angular velocity  $\Omega_0$  is used as the origin of a rotating Cartesian coordinate system in which  $x$ ,  $y$  and  $z$  correspond to the radial, azimuthal and vertical directions. The local shear rate in the disc is given by Oort’s first constant  $A_0 = -(r_0/2)(d\Omega/dr)_0$ . Having selected the reference point, we subsequently omit the subscript zero. We assume throughout that  $\Omega > A > 0$ ; in a Keplerian disc,  $A = \frac{3}{4}\Omega$ .

In this section, by way of introduction and for the sake of comparison with subsequent results, we consider a simple two-dimensional model without self-gravity, heating or cooling. We work with the equation of motion,

$$\Sigma(\partial_t u_i + u_j \partial_j u_i + 2\Omega \epsilon_{i3j} u_j) = -\Sigma \partial_i \Phi - \partial_i P + \partial_j \mathcal{T}_{ij}, \quad (1)$$

and the equation of mass conservation,

$$\partial_t \Sigma + \partial_i (\Sigma u_i) = 0, \quad (2)$$

where  $\Sigma$ ,  $P$ , and  $\mathcal{T}_{ij}$  are the vertically integrated density, pressure and viscous stress,  $u_i$  is the fluid velocity, and  $\Phi = -2\Omega A x^2$  is the tidal potential. The viscous stress is given by

$$\mathcal{T}_{ij} = \bar{\nu} \Sigma (\partial_i u_j + \partial_j u_i) + (\bar{\nu}_b - \frac{2}{3} \bar{\nu}) \Sigma (\partial_k u_k) \delta_{ij}, \quad (3)$$

where  $\bar{\nu}$  and  $\bar{\nu}_b$  are the vertically averaged kinematic viscosity and bulk viscosity. The basic state of the disc is given by  $u_y = -2Ax$ ,  $\Sigma = \text{constant}$ , and  $\mathcal{T}_{xy} = -2A\bar{\nu}\Sigma$ . We assume that  $P$ ,  $\bar{\nu}$ , and  $\bar{\nu}_b$  are specified functions of  $\Sigma$ , and define the sound speed  $v_s$  through  $v_s^2 = dP/d\Sigma$ .

We introduce perturbations of the form  $\text{Re}[\Sigma' \exp(st + ikx)]$ , etc., where  $s$  is the (complex) growth rate and  $k$  is the (real) radial wavenumber. These perturbations are independent of  $y$  and correspond to axisymmetric waves in cylindrical geometry, but also accurately describe the local properties of non-axisymmetric waves of modest azimuthal wavenumber in a thin disc. The linearized equations read

$$\Sigma(su'_x - 2\Omega u'_y) = -ikv_s^2 \Sigma' + ik\mathcal{T}'_{xx}, \quad (4)$$

$$\Sigma [su'_y + 2(\Omega - A)u'_x] = ik\mathcal{T}'_{xy}, \quad (5)$$

$$s\Sigma' + \Sigma iku'_x = 0, \quad (6)$$

$$\mathcal{T}'_{xx} = (\bar{\nu}_b + \frac{4}{3}\bar{\nu})\Sigma iku'_x, \quad (7)$$

$$\mathcal{T}'_{xy} = -2A\frac{d(\bar{\nu}\Sigma)}{d\Sigma}\Sigma' + \bar{\nu}\Sigma iku'_y. \quad (8)$$

Solution of this algebraic system yields the dispersion relation

$$s^3 + (\bar{\nu}_b + \frac{7}{3}\bar{\nu})k^2s^2 + [\Omega_r^2 + v_s^2k^2 + \bar{\nu}(\bar{\nu}_b + \frac{4}{3}\bar{\nu})k^4]s + 4\Omega A\frac{d(\bar{\nu}\Sigma)}{d\Sigma}k^2 + v_s^2k^2\bar{\nu}k^2 = 0, \quad (9)$$

where  $\Omega_r^2 = 4\Omega(\Omega - A)$  is the square of the radial epicyclic frequency, and is assumed to be positive. (The symbol  $\kappa$ , conventional for the epicyclic frequency, is used below to denote opacity.) In a Keplerian disc,  $\Omega_r = \Omega$ .

In the special case of an inviscid disc we obtain either a zero-frequency mode with  $s = 0$  and  $u'_x = 0$ , corresponding to a steady ‘geostrophic flow’ in which the Coriolis force is balanced by a pressure gradient, or an undamped inertial-acoustic wave with frequency  $\omega$  given by the familiar dispersion relation  $\omega^2 = -s^2 = \Omega_r^2 + v_s^2k^2$ .

Consider first the long-wavelength limit,  $k \rightarrow 0$ , of the dispersion relation. One root behaves according to

$$s = -\frac{4\Omega A}{\Omega_r^2}\frac{d(\bar{\nu}\Sigma)}{d\Sigma}k^2 + O(k^4), \quad (10)$$

which yields exponential growth (viscous instability) when

$$\frac{d(\bar{\nu}\Sigma)}{d\Sigma} < 0, \quad (11)$$

as found originally by Lightman & Eardley (1974). The other two roots have the behaviour

$$s = \pm i\Omega_r \left( 1 + \frac{v_s^2k^2}{2\Omega_r^2} \right) + \frac{1}{2} \left[ -(\bar{\nu}_b + \frac{7}{3}\bar{\nu}) + \frac{4\Omega A}{\Omega_r^2}\frac{d(\bar{\nu}\Sigma)}{d\Sigma} \right] k^2 + O(k^4). \quad (12)$$

This yields exponentially growing oscillations (viscous overstability) when

$$\frac{d(\bar{\nu}\Sigma)}{d\Sigma} > (\bar{\nu}_b + \frac{7}{3}\bar{\nu})\frac{\Omega_r^2}{4\Omega A}. \quad (13)$$

Now consider shorter wavelengths. If viscous instability occurs in the limit  $k \rightarrow 0$ , we reach marginal stability with  $s = 0$  when

$$\bar{\nu}v_s^2k^2 = -4\Omega A\frac{d(\bar{\nu}\Sigma)}{d\Sigma}. \quad (14)$$

Alternatively, if viscous overstability occurs in the limit  $k \rightarrow 0$ , we reach marginal stability with  $s = -i\omega \neq 0$  when

$$\begin{aligned} \bar{\nu}(\bar{\nu}_b + \frac{4}{3}\bar{\nu})(\bar{\nu}_b + \frac{7}{3}\bar{\nu})k^4 + (\bar{\nu}_b + \frac{4}{3}\bar{\nu})v_s^2k^2 \\ = 4\Omega A\frac{d(\bar{\nu}\Sigma)}{d\Sigma} - (\bar{\nu}_b + \frac{7}{3}\bar{\nu})\Omega_r^2. \end{aligned} \quad (15)$$

In each case the right-hand side of the equation is positive while the left-hand side is a monotonically increasing function of  $k^2$ , vanishing at  $k^2 = 0$ , so we find a unique positive value of  $k^2$  for marginal stability. The instability or overstability is quenched for all shorter wavelengths.

For example, a Keplerian disc with constant kinematic shear viscosity  $\bar{\nu} \ll v_s^2/\Omega$  and no bulk viscosity exhibits

the viscous overstability on wavelengths  $\gtrsim 9v_s/\Omega$ , while the maximum growth rate occurs for a wavelength  $\approx 13v_s/\Omega$ . These wavelengths are several times the disc thickness, partly because the case of constant  $\bar{\nu}$  is close to marginal stability. We presume that the reason that the overstability is rarely or never observed in two-dimensional numerical simulations that include an explicit shear viscosity is either that the domain is too small or the numerical method has an effective bulk viscosity. (Shearing-box simulations of turbulent discs are invariably too small in the radial direction to detect any overstability.)

The shearing-sheet approximation is valid only for wavenumbers satisfying  $|kr| \gg 1$ . For wavelengths comparable to  $r$ , not only must the effects of cylindrical geometry be considered but also the global structure of the disc and the radial boundary conditions. For our purposes, the shearing sheet correctly describes the local properties of waves in discs.

### 3 THREE-DIMENSIONAL MODEL

Our full treatment is based on a three-dimensional shearing sheet. We omit self-gravity but include viscous heating and radiative cooling.

#### 3.1 Basic equations

We work with the equation of motion,

$$\rho(\partial_t u_i + u_j \partial_j u_i + 2\Omega \epsilon_{ij3} u_j) = -\rho \partial_i \Phi - \partial_i p + \partial_j T_{ij}, \quad (16)$$

the equation of mass conservation,

$$\partial_t \rho + \partial_i (\rho u_i) = 0, \quad (17)$$

and the thermal energy equation,

$$(\gamma - 1)^{-1}(\partial_t p + u_i \partial_i p + \gamma p \partial_i u_i) = T_{ij} \partial_i u_j - \partial_i F_i, \quad (18)$$

where

$$T_{ij} = \mu(\partial_i u_j + \partial_j u_i) + (\mu_b - \frac{2}{3}\mu)(\partial_k u_k)\delta_{ij} \quad (19)$$

is the viscous stress ( $\mu$  and  $\mu_b$  being the dynamic shear and bulk viscosities),  $\Phi = -2\Omega Ax^2 + \frac{1}{2}\Omega_z^2 z^2$  is the tidal potential ( $\Omega_z$  being the vertical epicyclic frequency, equal to  $\Omega$  in a Keplerian disc),

$$F_i = -\frac{16\sigma T^3}{3\kappa\rho}\partial_i T \quad (20)$$

is the radiative energy flux density, and the other symbols have their usual meanings. We assume an ideal gas with equation of state  $p = R\rho T$  and with  $\gamma = \text{constant}$ . The properties  $\mu$ ,  $\mu_b$  and  $\kappa$  are regarded as functions of  $\rho$  and  $T$ .

#### 3.2 Equilibrium disc

The basic state of the disc is given by  $u_y = -2Ax$ ,  $\rho = \rho(z)$ ,  $T = T(z)$ ,  $T_{xy} = -2A\mu$ , and  $F_z = F_z(z)$ . For hydrostatic equilibrium,

$$\partial_z p = \rho g_z = -\rho \Omega_z^2 z, \quad (21)$$

and for thermal equilibrium,

$$\partial_z F_z = 4A^2\mu. \quad (22)$$

These conditions are solved together with the constitutive relations to determine the equilibrium model. We adopt the ‘zero boundary conditions’ whereby  $\rho = T = 0$  at the surfaces  $z = \pm H$  of the disc. These are appropriate to describe an optically thick disc and avoid the complications of matching to an atmospheric model. The surface density is

$$\Sigma = \int_{-H}^H \rho \, dz, \quad (23)$$

and we define the vertically averaged kinematic viscosity  $\bar{\nu}$  (and analogously  $\bar{\nu}_b$ ) via

$$\bar{\nu}\Sigma = \int_{-H}^H \mu \, dz. \quad (24)$$

Under convenient assumptions the problem can be reduced to a standard dimensionless form (Ogilvie 2001). Let the viscosity be given by  $\mu = \alpha p / \Omega$  and  $\mu_b = \alpha_b p / \Omega$ , where  $\alpha$  and  $\alpha_b$  are dimensionless constants, and let  $\kappa = C_\kappa \rho^X T^Y$ , where  $C_\kappa$ ,  $X$  and  $Y$  are constants. In particular, for Thomson (electron scattering) opacity,  $X = Y = 0$ . The method of solution for the vertical structure is described in Appendix A, where it is shown that  $\bar{\nu}\Sigma \propto \Sigma^{(10+3X-2Y)/(6+X-2Y)}$ .

### 3.3 Linearized equations

As in Section 2, we introduce axisymmetric perturbations of the form  $\text{Re}[\rho'(z) \exp(st + ikx)]$ , etc., and obtain the linearized equations

$$\rho(su'_x - 2\Omega u'_y) = -ikp' + ikT'_{xx} + \partial_z T'_{xz}, \quad (25)$$

$$\rho[su'_y + 2(\Omega - A)u'_x] = ikT'_{xy} + \partial_z T'_{yz}, \quad (26)$$

$$\rho su'_z = \rho' g_z - \partial_z p' + ikT'_{xz} + \partial_z T'_{zz}, \quad (27)$$

$$sp' + u'_z \partial_z \rho + \rho \Delta = 0, \quad (28)$$

$$sp' + u'_z \partial_z p + \gamma p \Delta = \mathcal{N}, \quad (29)$$

with

$$\Delta = iku'_x + \partial_z u'_z, \quad (30)$$

$$\mathcal{N} = (\gamma - 1)(-2AT'_{xy} + T_{xy}iku'_y - ikF'_x - \partial_z F'_z), \quad (31)$$

$$T'_{xx} = 2\mu iku'_x + (\mu_b - \frac{2}{3}\mu)\Delta, \quad (32)$$

$$T'_{xy} = -2A\mu' + \mu iku'_y, \quad (33)$$

$$T'_{xz} = \mu(iku'_z + \partial_z u'_x), \quad (34)$$

$$T'_{yz} = \mu \partial_z u'_y, \quad (35)$$

$$T'_{zz} = 2\mu \partial_z u'_z + (\mu_b - \frac{2}{3}\mu)\Delta, \quad (36)$$

$$F'_x = -\frac{16\sigma T^3}{3\kappa\rho} ikT', \quad (37)$$

$$F'_z = -\frac{16\sigma T^3}{3\kappa\rho} \left\{ \partial_z T' + \left[ -(1+X)\frac{\rho'}{\rho} + (3-Y)\frac{T'}{T} \right] \partial_z T' \right\}, \quad (38)$$

$$\frac{T'}{T} = \frac{p'}{p} - \frac{\rho'}{\rho}, \quad (39)$$

$$\mu' = \frac{\alpha p'}{\Omega}. \quad (40)$$

Note that  $\mathcal{N}$  represents the effects of non-adiabatic heating and cooling.

In general this eighth-order system of ordinary differential equations must be solved numerically as an eigenvalue problem for the growth rate  $s$ , with the wavenumber  $k$  as a real parameter. The boundary conditions are that the solution should be regular at the surfaces  $z = \pm H$ , which are singular points of the differential equations. The numerically determined solutions  $s(k)$  define the various branches of the dispersion relation of the disc.

If equations (25)–(29) are solved with the stress perturbations  $T'_{ij}$  and the non-adiabatic term  $\mathcal{N}$  set to zero, we have a self-adjoint eigenvalue problem of the kind solved by Korycansky & Pringle (1995). Indeed the structure of an optically thick disc with zero boundary conditions is very similar to that of a polytropic disc. We refer to this as the ‘inviscid problem’.

### 3.4 Integral relation

Using the preceding set of linearized equations and carrying out various integrations by parts, we obtain the integral relation

$$\begin{aligned} -s^2 \int_{-H}^H \rho (|u'_x|^2 + |u'_z|^2) \, dz = & \int_{-H}^H \left\{ \rho \Omega_r^2 |u'_x|^2 + \rho N^2 |u'_z|^2 + \frac{1}{\gamma p} |u'_z \partial_z p + \gamma p \Delta|^2 \right. \\ & - \Delta^* \mathcal{N} + 2s\mu (|iku'_x - \frac{1}{3}\Delta|^2 + \frac{1}{2}|iku'_z + \partial_z u'_x|^2 \\ & + |\partial_z u'_z - \frac{1}{3}\Delta|^2 + |\frac{1}{3}\Delta|^2) + s\mu_b |\Delta|^2 \\ & - \left( \frac{\Omega}{\Omega - A} \right) \frac{1}{\rho} |ikT'_{xy} + \partial_z T'_{yz}|^2 - s^* \left( \frac{\Omega}{\Omega - A} \right) \\ & \left. \times (\mu k^2 |u'_y|^2 + \mu |\partial_z u'_y|^2 + 2A\mu' iku'_y) \right\} dz, \end{aligned} \quad (41)$$

where

$$N^2 = g_z \left( \partial_z \ln \rho - \frac{1}{\gamma} \partial_z \ln p \right) \quad (42)$$

is the square of the Brunt–Väisälä frequency. This relation is closely related to equation (13) in Kley et al. (1993). In the absence of viscous and non-adiabatic effects, it yields a real integral expression for the squared frequency  $\omega^2 = -s^2$  of the mode, which has the usual variational property associated with self-adjoint eigenvalue problems. More generally, the imaginary part of this equation yields (with  $s = s_r + is_i$ )

$$\begin{aligned} s_r \int_{-H}^H \rho (|u'_x|^2 + |u'_z|^2) \, dz & = \frac{1}{2s_i} \text{Im} \int_{-H}^H \left[ \Delta^* \mathcal{N} + s^* \left( \frac{\Omega}{\Omega - A} \right) 2A\mu' iku'_y \right] dz \\ & - \int_{-H}^H \left\{ \mu (|iku'_x - \frac{1}{3}\Delta|^2 + \frac{1}{2}|iku'_z + \partial_z u'_x|^2 \right. \\ & + |\partial_z u'_z - \frac{1}{3}\Delta|^2 + |\frac{1}{3}\Delta|^2) + \frac{1}{2}\mu_b |\Delta|^2 \\ & \left. + \left( \frac{\Omega}{\Omega - A} \right) \frac{1}{2}\mu (k^2 |u'_y|^2 + |\partial_z u'_y|^2) \right\} dz. \end{aligned} \quad (43)$$

Within the first integral on the right-hand side, the first term quantifies non-adiabatic effects, while the second quantifies those of the underlying stress variation. The second integral on the right-hand side represents viscous dissipation. We rewrite the equation as

$$s_r = N + S + D, \quad (44)$$

where  $N$ ,  $S$ , and  $D$  represent the three effects.

This relation is similar to equation (3.7) of Kato (1978) but is considerably more general because it does not assume that the mode is only slightly perturbed from a solution of the inviscid problem. It shows that there are two effects that can promote growth of the wave. One is the non-adiabatic term  $N$ , if it is appropriately correlated with the velocity divergence  $\Delta$ . (This effect is similar to the mechanism of thermal overstability in stars.) The other is the viscosity perturbation  $\mu'$  (which derives from the stress perturbation  $T'_{xy}$ ), if it is appropriately correlated with the azimuthal velocity perturbation  $u'_y$ . (This is the mechanism of viscous overstability.) These two potentially positive contributions must compete with a number of negative definite terms which correspond to the damping effect of the unperturbed viscosity acting on the shear that is present in the mode. It is evident from this competition that modes with the least complicated vertical structure, such as the  $f^e$  mode, are the most likely to be overstable.

### 3.5 Long-wavelength behaviour

In Appendix B we present an asymptotic analysis of waves in the long-wavelength limit,  $k \rightarrow 0$ , in the presence of viscosity. In this limit most of the modes have a damping rate  $-\text{Re}(s)$  comparable to  $\alpha\Omega$ . Of those that do not, one behaves according to equation (10) and therefore yields the same criterion for viscous instability as in the two-dimensional theory. It does so because, to a first approximation, the wave does not disturb the hydrostatic and thermal balances present in the unperturbed disc.

The remaining long-wavelength solutions have a dispersion relation of the form

$$s = \pm i\Omega_r + s_2 k^2 + O(k^4), \quad (45)$$

where the constant  $s_2$  is determined by an algebraic problem derived in Appendix B. These waves yield a criterion for viscous overstability,  $\text{Re}(s_2) > 0$ , that differs from the prediction of the two-dimensional analysis. The differences arise because the wave has an (epicyclic) period comparable to the time-scales for establishing the hydrostatic and thermal balances, and the vertical structure of the disc therefore requires a dynamical treatment. Vertical motion, in the form of a ‘breathing motion’ with  $u'_z \propto z$ , plays a significant role in the dynamics of this mode. The overstability criterion for a Keplerian disc derived by this method agrees exactly with that found by the method of Ogilvie (2001), who also noted the importance of vertical motion and non-equilibrium.

As an example, for a Keplerian disc with constant (e.g. Thomson) opacity and  $\alpha, \alpha_b \ll 1$ , overstability occurs for

$$\alpha_b/\alpha < (-33\gamma^2 + 138\gamma - 97)/12. \quad (46)$$

In contrast, the two-dimensional analysis (using the result that  $\bar{\nu}\Sigma \propto \Sigma^{5/3}$  for the case of constant opacity) predicts

overstability for  $\alpha_b/\alpha < 8/3$ . When  $\gamma = 5/3$ , the three-dimensional disc is more susceptible to overstability, as then the right-hand side equals  $31/9 \approx 3.44$ .

### 3.6 Modelling the turbulent stress

As the ordinary molecular viscosity is too small to be appreciable, the viscous stress is presumably of turbulent origin. The simplest ‘closure’ model, and the one we have adopted here, is the alpha prescription, which assumes a Newtonian stress-strain relation and an isotropic effective viscosity. However, both assumptions are likely to be poor approximations, because the turbulent stress (probably of magnetohydrodynamic origin) should have a non-zero relaxation time comparable to the orbital period, and the effective viscosity may be considerably anisotropic. In principle we could apply a more sophisticated closure (e.g. Ogilvie 2001, 2003), but doing so may raise more questions, and in fact obscure essential physics that is model-independent. It hence pays to examine the simpler alpha model disc first in detail. In this context the bulk viscosity is deployed mainly as a surrogate for whatever stabilizing influences (e.g. stress relaxation) may act against overstability in reality.

## 4 NUMERICAL ANALYSIS

We seek growing modes on general radial length-scales in a vertically stratified gaseous disc with small viscosity. This task requires the solution of two boundary-value problems. The first determines the vertical structure of the disc equilibrium (Appendix A, equations A6–A10), while the second determines the vertical structure of the linear modes (Section 3.3, equations 25–40). For simplicity and clarity we adopt a constant (e.g. Thomson) opacity model and assume the disc is Keplerian; thus  $X = Y = 0$ ,  $\Omega_z/\Omega = 1$  and  $A/\Omega = 3/4$ . Furthermore, the adiabatic exponent,  $\gamma$ , is set equal to either  $7/5$  or  $5/3$ . Hence the main parameters to vary are  $\alpha$  and  $\alpha_b$  (the shear and bulk viscosities) and  $k$  (the radial wavenumber). The regimes in which we are interested require these to be small.

Two numerical methods were employed: the ‘shooting method’ and Chebyshev collocation. The former method was used to solve the nonlinear equilibrium equations. The latter method represents the ODEs of the linear system on a Gauss–Lobatto grid and requires solution of a generalized algebraic eigenvalue problem. As the equations possess a singularity at the upper boundary, both methods were supplemented at this point by an asymptotic analysis in order to determine the correct limiting behaviour. A judicious choice of dependent variables was also necessary in both cases. The midplane boundary conditions follow from symmetry considerations. For example, even modes require  $u'_z = du'_x/dz = du'_y/dz = dp'/dz = 0$  at  $z = 0$ .

In addition, we set the ‘shooting method’ upon the linearised perturbation equations, so as to check the results of the Chebyshev collocation method. For modest values of  $\alpha$  and  $k$  the agreement between them was good. However, for  $k$  and  $\alpha$  in the parameter regime of greatest interest, the ‘shooting method’ either failed to converge to the overstable mode or settled on an eigenpair numerically ‘contaminated’ by a nearby mode. This we blame on the stiffness of the

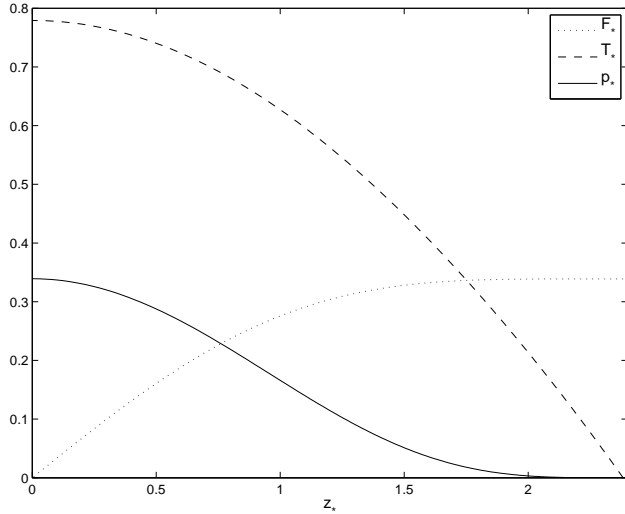


**Figure 1.** Non-dimensionalized pressure,  $p_*$ , vertical radiative flux,  $F_*$ , and temperature,  $T_*$ , as functions of non-dimensionalized height,  $z_*$ , for an equilibrium disc with constant opacity ( $X = Y = 0$ ).

equations in this regime. The collocation method did not encounter this difficulty. It, however, could produce eigenpairs which were spurious or unconverged, and these required winnowing out. Also, when examining very long waves for low viscosities, Chebyshev collocation suffered from numerical error, which often compromised accurate determination of the growth rate, these being typically  $O(\alpha k^2)$ . That said, on scales for which interesting behaviour occurred, this was not an issue: with twenty Gauss–Lobatto nodes the overstable growth rate had converged to ten significant figures.

We present in the following section:

- (i) the vertical structure of the equilibrium (Fig. 1);
- (ii) the behaviour of the overstable mode's growth rate as a function of  $k$  for different  $\alpha$  and  $\gamma$ , when  $\alpha_b = 0$ , alongside the components of the integral relation (44) in each case (Figs 2–4);
- (iii) eigenfunction structures for two illustrative parameter regimes (Figs 5 and 6); and
- (iv) the critical ratios of  $\alpha_b$  and  $\alpha$  for the onset of over-stability (Figs 7 and 8).

## 5 RESULTS

### 5.1 Equilibrium

The characteristic structure of the equilibrium state, which we plot in Fig. 1, differs little from a polytropic model, except for the addition of the vertical heat flux, which is necessarily zero at the midplane and approaches a constant on the boundary. This constant and the semithickness of the disc serve as the ‘eigenvalues’ of the boundary value problem and take the approximate values 0.34 and 2.4 for the case considered ( $X = Y = 0$ ).

### 5.2 Growth rates and eigenfunctions

We present the solution of the non-dimensionalized versions of equations (25)–(40), in which  $s = s_*\Omega$ ,  $k = k_*/U_H$ ,  $u'_i = u'_{i*}\Omega U_H$ , while  $\rho'$ ,  $p'$ ,  $T'$ , and  $F'_i$  take the same units as their equilibrium counterparts (see Appendix A). Since  $H \approx 2.4 U_H$ , a wavenumber  $k = 1$  corresponds to a wavelength approximately 1.3 times the full disc thickness  $2H$ . The growth rate is expressed in terms of the orbital frequency, the inverse of the dynamical time-scale. The stars will be dropped for the rest of this section.

Amongst the various even modes exhibited by the disc, our numerical method found that only one has the potential to grow: as expected, the viscous analogue of the inviscid  $f^e$  mode, in the interval  $0 < k < 1$ . No mode of odd symmetry grows.

In Fig. 2a we plot the real part of the growth rate of the overstable mode, scaled by  $k^2$ , for modest shear viscosity and no bulk viscosity. As  $k \rightarrow 0$ , this quantity approaches a constant value approximately equal to 0.0459, the same value predicted by the long-wavelength theory (cf. equation B45). On short enough scales,  $k \sim 1$ , the mode ceases to grow. Qualitatively this behaviour mirrors that of the two-dimensional model.

In Fig. 2b we plot the components of the integral relation (44), the competition of which establishes growth or decay on the various scales. Immediately we note that the non-adiabatic effects, embodied in the term  $\mathbf{N}$ , are an order smaller than those of viscous dissipation,  $\mathbf{D}$ , and stress variation,  $\mathbf{S}$ . On long horizontal scales  $\mathbf{N}$  contributes to overstability, presumably through a variant of the  $\epsilon$ -mechanism in stars, resulting here from the increase of viscous dissipation in the compressed phase of the oscillation. But on sufficiently small horizontal scales, thermal diffusion dominates  $\mathbf{N}$  and acts to smooth out disturbances ( $\mathbf{N} < 0$ ). Overstability is due almost entirely to the stress variation, which competes with viscous damping. This competition is most likely to succeed on the longest wavelengths, where the mode is dominated by horizontal motion and can avoid vertical shear. In this regime, weak viscous forces are sufficient to allow the mode to deviate from the natural form of the inviscid  $f^e$  mode. On shorter wavelengths, however, the horizontal motion necessarily develops vertical shear and is accompanied by vertical motion, making the stress variation less efficient in driving overstability. The increasing horizontal shear also acts to suppress the overstability.

When  $\alpha$  is an order smaller or less, the prevalence of overstability on the various scales becomes more complicated, as Figs 3 and 4 reveal. Three characteristic length-scales emerge, which may be divided into:

- (i) the long-wavelength limit (described in Section 3.5):  $0 < k \lesssim \alpha \ll 1$ ;
- (ii) an intermediate regime of anomalous viscous dissipation, and, consequently, stability:  $0 < \alpha \ll k \ll 1$ ; and
- (iii) a regime on shorter scales,  $0 < \alpha \ll k \sim 1$ , in which overstability may reappear.

In the long-wavelength regime, the overstable mode minimizes the amount of vertical shear in the horizontal motion (and hence  $\mathbf{D}$ ) by maintaining  $u'_x$  and  $u'_y$  effectively constant with respect to  $z$  (Fig. 5b). But as  $k$  increases, the variation of  $u'_x$  and  $u'_y$  with  $z$  increases until, by  $k \gtrsim \alpha^{1/2}$ , they

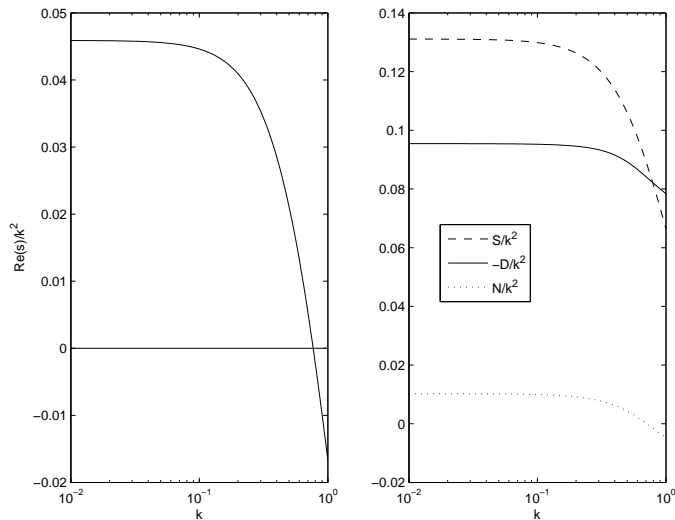


**Figure 2.** (a) Real part of the growth rate of the overstable mode divided by  $k^2$ , as a function of  $k$ , for  $\alpha = 0.1$ ,  $\alpha_b = 0$ ,  $X = Y = 0$  and  $\gamma = 7/5$ . The curve asymptotes to a value  $\approx 0.0459$  as  $k \rightarrow 0$ . The growth rate  $s$  is in units of  $\Omega$ , and the wavenumber  $k$  is in units of  $U_H^{-1}$  as described at the beginning of Section 5.2. (b) Components of the integral relation (44).  $S$  refers to the stress variation contribution,  $N$  to the non-adiabatic contribution, and  $D$  to viscous dissipation.

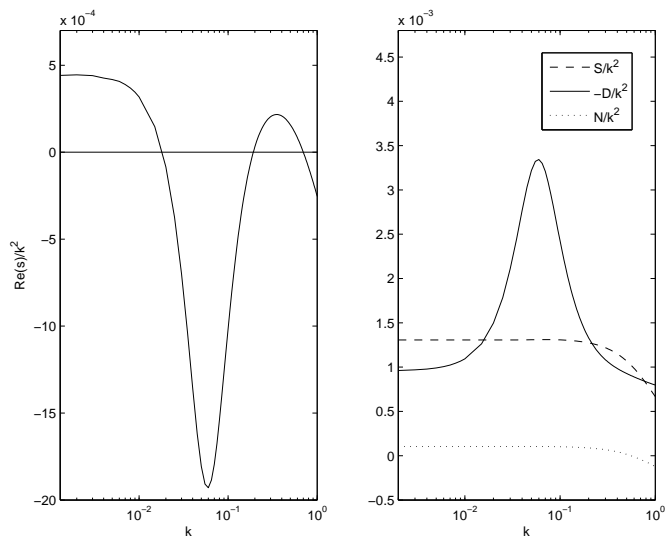


**Figure 3.** As for Fig. 2 but with  $\alpha = 0.001$ ,  $\alpha_b = 0$ ,  $X = Y = 0$  and  $\gamma = 7/5$ . Note the interval of intermediate length-scales which are stable.

resemble the eigenfunctions of the inviscid problem (Fig. 6). This complication in the mode's vertical structure leads to greater viscous dissipation and, subsequently, decay. However, once the mode has assumed the limiting form of the inviscid eigenfunction, the amount of shear 'saturates'. Consequently, the viscous dissipation plateaus, and on shorter scales overstability may appear again. The viscous stress in this third regime may be considered a small perturbation to the inviscid equations, along the lines of Kato (1978), the principal difference being that Kato assumed that the

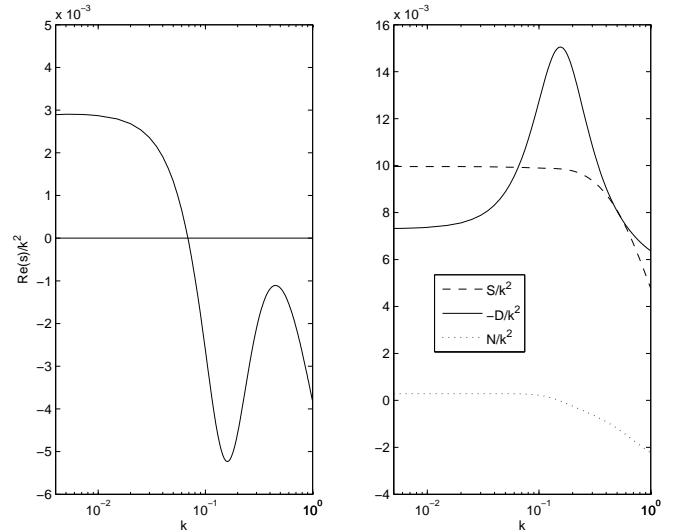


**Figure 4.** As for Fig. 2 but with  $\alpha = 0.007$ ,  $\alpha_b = 0$ ,  $X = Y = 0$  and  $\gamma = 5/3$ . Note that for larger  $\gamma$ , all intermediate wavelengths are stable.

perturbation was with respect to a mode with no vertical shear.

We find that the imaginary part of the growth rate is unaffected by the increase in viscous dissipation when  $\alpha$  is small. The long-wavelength theory correctly predicts the  $O(k^2)$  correction up until intermediate scales. This result implies that the group velocity of the  $f^e$  mode, and in particular that determining the propagation of eccentricity in discs, is described accurately by the three-dimensional long-wavelength theory.

Odd modes require that the horizontal components of the motion are zero at the midplane. This means that if such modes are to minimize their vertical shear, and hence avoid the destructive effects of viscous dissipation,  $u'_x$  and  $u'_y$  must remain near zero throughout the disc. But doing so will stall the mechanism driving overstability, as it requires a healthy correlation between  $u'_y$  and  $\mu'$ . This partly explains why only even modes exhibit overstability.

For  $k \sim 1$ , a larger  $\gamma$  may quench overstability (Fig. 4), whereas with long wavelengths a larger  $\gamma$  generally stimulates overstability, as equation (46) shows. The latter behaviour originates in  $\gamma$ 's enhancement of the pressure perturbation in the  $S$  term, which, according to the long wavelength theory, proceeds from its dependence on  $W$  (cf. equation B37). For low viscosities, the adiabatic index controls the magnitude of the vertical breathing motion via  $|W/U| = (\gamma - 1)/\gamma$ . Thus a larger  $\gamma$  produces a larger  $W$ , larger vertical pressure advection, and consequently a larger  $S$ . This effect appears more important than enhanced viscous dissipation arising from the increase in vertical motion.

When  $k \sim 1$ , the mode's response to variations in  $\gamma$  may be broken into two components. Firstly, an increase in  $\gamma$  increases the scale upon which  $N$  becomes negative: thermal diffusion begins to stabilize the mode for smaller  $k$ . And, in fact, when  $\gamma$  is sufficiently large, the non-adiabatic term is always negative. This behaviour springs from the sensitivity to  $\gamma$  of the radiative damping terms in  $\mathcal{N}$  (cf. equation 31). This may arise from their dependence on  $T'$ , which

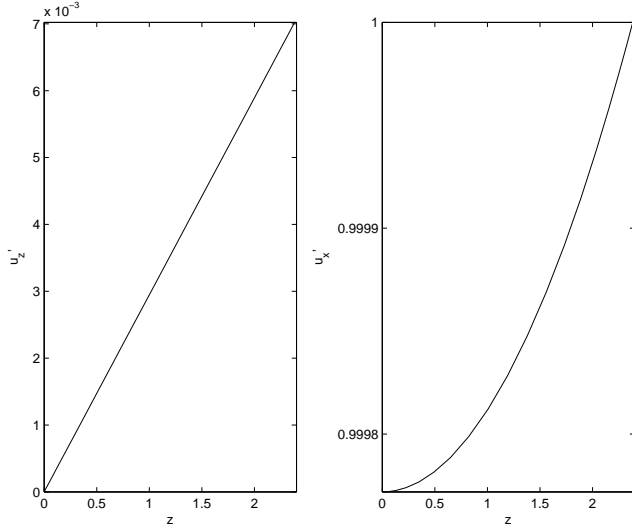


**Figure 5.** The  $u'_z$  and  $u'_x$  structure of the overstable mode for  $\alpha = 0.1$ ,  $k = 0.01$ ,  $\gamma = 7/5$  and  $\alpha_b = X = Y = 0$ . The eigenfunction has been normalized so that  $u'_x = 1$  at the boundary. As predicted by the long-wavelength theory,  $u'_z$  is linear in  $z$  and is  $O(k)$ , while the  $u'_x$  eigenfunction is composed of an  $O(1)$  constant component and an  $O(k^2)$  varying component.

is larger for larger  $\gamma$  (while the other non-adiabatic contributions, and  $\Delta$ , do not vary significantly). Presumably, if the opacity is non-constant ( $X, Y$  non-zero) a version of the  $\kappa$ -mechanism of overstability in stars may arise, though we do not explore that here.

Secondly, and more importantly, an increase in  $\gamma$  may contribute to an increase in the amount of shear in the horizontal velocities, by analogy with the inviscid problem. This arises via  $\gamma$ 's influence on the vertical stratification of the disc, and the enhanced buoyancy forces which ensue. Lubow & Pringle (1993) established analytically that the related ‘two-dimensional mode’ in an inviscid isothermal disc possesses  $u'_x$  and  $u'_y$  which are  $\propto \exp(N^2/\Omega_z^2) = \exp[(\gamma - 1)(z/H)^2/\gamma]$ . More generally, the amount of shear in the horizontal motions of an even inviscid p or f mode increases with  $N^2$  and  $z$  (see equation 13 in Korycansky & Pringle 1995).

### 5.3 Stability curves

Now we let  $\alpha_b$  vary. Since  $\alpha_b$  has a purely stabilizing effect on the mode, a unique (but possibly negative) critical value  $(\alpha_b/\alpha)_c$  for marginal overstability can be identified for given values of  $\alpha$ ,  $\gamma$  and  $k$ . The smaller the value of  $(\alpha_b/\alpha)_c$ , the more likely that the overstability is suppressed by stabilizing influences such as turbulent stress relaxation. The resulting curves of marginal stability we plot in Figs 7 and 8, for  $\alpha = 0.1$  and  $\alpha = 0.001$  respectively.

Both plots verify the predictions of the long-wavelength theory when  $\alpha$  is small: as  $k \rightarrow 0$ ,  $(\alpha_b/\alpha)_c \rightarrow 195/75$  (equation 46), when  $\gamma = 7/5$ . Also, for sufficiently small  $\alpha$ , the scales divide into the three regimes we explored earlier (Fig. 8). We find that for small  $\alpha$  and  $k \sim 1$  the marginal curves converge to a limiting curve, differing very little from that appearing in Fig. 8. This confirms that the stress in this

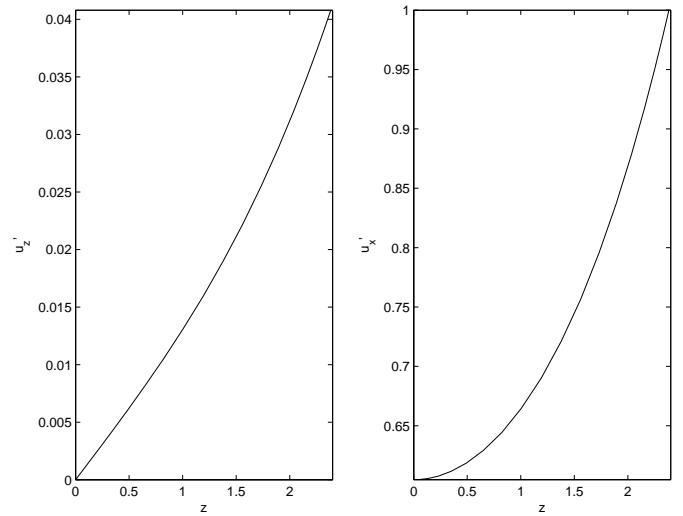


**Figure 6.** The  $u'_z$  and  $u'_x$  vertical structure for  $\alpha = 0.001$ ,  $k = 0.1$ ,  $\gamma = 7/5$  and  $\alpha_b = X = Y = 0$ . The eigenfunction resembles the f<sup>e</sup> mode of the inviscid problem, and decays for these parameters.

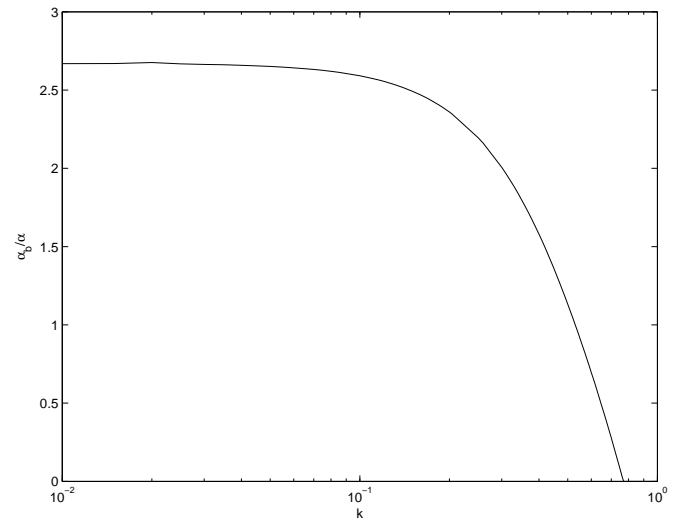


**Figure 7.** Curve of marginal viscous overstability in the  $(k, \alpha_b/\alpha)$  plane for  $\alpha = 0.1$  and  $\gamma = 7/5$ . The region above the curve is stable. As predicted by the long-wavelength theory, the curve approaches  $197/75 \approx 2.627$  as  $k \rightarrow 0$ .

regime behaves like a regular perturbation upon the inviscid problem.

What is interesting is the relative difficulty overstability encounters in the third regime,  $k \sim 1$ , when bulk viscosity is added. An  $\alpha_b$  a little larger than  $\alpha$  is enough to quench overstability, whereas longer waves require a value more than twice  $\alpha$ . We conclude that overstability on shorter scales is relatively fragile: a smaller  $\alpha_b$  will switch it off (as will increasing  $\gamma$ ). This is despite the fact that unstable modes in this regime will grow far more vigorously than those on the longer scales. The simulations of Kley et al. (1993) reflect this behaviour. The largest radial lengthscale resolvable in their model was approximately  $10H$ , which falls comfortably in the intermediate- to short-scale regime of our analysis. For



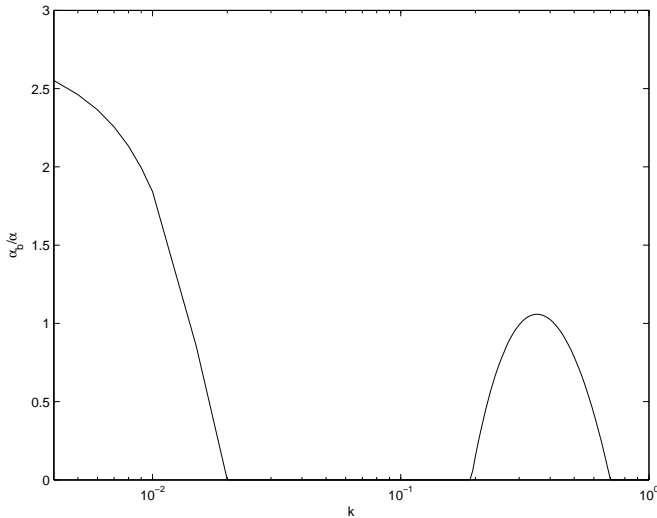


**Figure 8.** Curve of marginal viscous overstability in the  $(k, \alpha_b/\alpha)$  plane for  $\alpha = 0.001$  and  $\gamma = 7/5$ . The region above the curve is stable.

sufficiently small  $\alpha$ , intermediate- and short-scales will be stable for appropriate  $\gamma$  and/or  $\alpha_b$ . But, as  $\alpha$  increases and we leave the low-viscosity regime, these scales may become overstable, as Kley et al. report.

## 6 SUMMARY AND DISCUSSION

We have investigated the growth or decay rate of the fundamental mode of even symmetry in a three-dimensional viscous accretion disc. Our numerical model resolves the vertical structure of the disc and its modes, treating radiative energy transport in the diffusion approximation. Overstability can occur, in principle, for radial wavelengths longer than a few times the disc thickness. It results almost entirely from the fact that the unperturbed disc necessarily has a shear stress in order to facilitate accretion, and the variation of this stress in the wave motion allows energy to be fed from the differential rotation into growing oscillations. This tendency competes with the viscous damping of the mode. Smaller contributions to the growth rate arise from non-adiabatic effects related to the  $\epsilon$ - and  $\kappa$ -mechanisms in stars, and thermal diffusion.

The pattern of behaviour in a low-viscosity disc ( $\alpha \ll 1$ ) is as follows. For radial wavenumbers  $kH \sim 1$  (i.e. radial wavelengths a few times the disc thickness) the structure of the  $f^e$  mode resembles its counterpart in an inviscid disc. It has a non-trivial vertical structure dictated by the stratification of the disc; the horizontal velocities involve vertical shear and are accompanied by vertical motion. The mode can be overstable in this short-wavelength regime, depending on the parameters of the disc, but the presence of vertical shear and vertical motion acts against this tendency.

For very long radial wavelengths ( $kH \lesssim \alpha$ ) the mode is dominated by horizontal motion and the vertical shear is removed by the action of viscous stresses between different strata in the disc. This type of motion is optimal for exciting the overstability but the (complicated) analytical criterion we obtain in this regime differs from the prediction of a

two-dimensional model because the disc is not in vertical hydrostatic or thermal balance.

On intermediate wavelengths ( $\alpha \ll kH \ll 1$ ) a transitional behaviour is found. Here the vertical shear developing in the horizontal velocity perturbations leads to an enhanced viscous damping and the overstability is suppressed.

In order to bring out this subtle behaviour, we have restricted our attention in this paper to viscous models of accretion discs based on the Navier–Stokes equation and the alpha viscosity prescription. We fully appreciate that stress in accretion discs is likely to arise from magnetohydrodynamic turbulence and to exhibit a more complicated rheology (e.g. Ogilvie 2001, 2003). In particular, the non-zero relaxation time of the stress is known to act against the overstability (Ogilvie 2001) as it does in planetary rings (Latter & Ogilvie 2006). In this paper we have employed a bulk viscosity as a convenient surrogate for any such stabilizing tendencies.

A major application of this work is to the theory of eccentric accretion discs, since a small eccentricity can be regarded as a wave of azimuthal wavenumber  $m = 1$  and long radial wavelength propagating in a circular disc. Indeed, it is only for  $m = 1$  waves in (nearly) Keplerian discs that a long radial wavelength can be maintained over an extended radial distance. Overstability appears as a negative diffusion coefficient for eccentricity in the theory of Ogilvie (2001), which uses approximations similar to the long-wavelength regime described above. The approximations break down for intermediate wavelengths in a very low-viscosity disc, because the viscous stresses are inadequate to couple the different strata and enforce uniformity of the eccentricity with height.

While the overstability may be suppressed by stress relaxation effects, as suggested by Ogilvie (2001), an alternative possibility is that overstability may indeed occur on very long radial wavelengths, while shorter wavelengths require a treatment similar to that carried out here.

In protoplanetary discs the stress is of uncertain origin, but values in the range  $10^{-4} \lesssim \alpha \lesssim 10^{-2}$  are usually quoted based on observed accretion rates and disc lifetimes, while the angular semithickness is in the range  $0.05 \lesssim H/r \lesssim 0.1$ . In this case the long-wavelength analysis has no application, since the relevant wavelengths greatly exceed the size of the disc. Instead, the regimes of short and intermediate wavelengths describe the behaviour of global eccentric modes. This means that a correct determination of the damping rate of eccentricity in a protoplanetary system requires a three-dimensional treatment of the disc, allowing for vertical shear in the horizontal velocities. We find that a typical decay rate of a global eccentric mode (with a radial wavelength of  $20H$ ) is  $10^{-5} \Omega^{-1}$  for  $\alpha = 10^{-3}$  and  $2 \times 10^{-6} \Omega^{-1}$  for  $\alpha = 10^{-4}$ . These are only rough estimates as we have not considered the opacity regimes relevant to protoplanetary discs. For  $\alpha = 10^{-2}$  global modes may be overstable.

In other accretion discs  $H/r$  may be much smaller and  $\alpha$  somewhat larger. In this case the long-wavelength regime applies to global eccentric modes. The fact that the overstability is suppressed for intermediate wavelengths means that only the largest-scale modes may be permitted to grow. This would neatly account for the occurrence of global eccentric modes in accretion discs around Be stars.

No modes other than the  $f^e$  mode were found to exhibit

overstability. In particular, a similar mechanism would not permit global warping of discs to be excited.

## ACKNOWLEDGMENTS

HNL would like to acknowledge the funding of the Cambridge Commonwealth Trust.

## REFERENCES

- Borderies, N., Goldreich, P., Tremaine, S., 1985, *Icarus* 63, 406  
 Bate, M. R., Ogilvie, G. I., Lubow, S. H., Pringle, J. E., 2002, *MNRAS* 332, 575  
 Eddington, A. S., 1926, *The Internal Constitution of the Stars*, Cambridge Univ. Press, Cambridge  
 Goldreich, P., Lynden-Bell, D., 1965, *MNRAS* 130, 125  
 Kato, S., 1978, *MNRAS* 185, 629  
 Kato, S., 1983, *PASJ* 35, 249  
 Kato, S., Fukue, J., 1980, *PASJ* 32, 377  
 Kato, S., Honma, F., Matsumoto, R., 1988, *MNRAS* 231, 37  
 Kley, W., Papaloizou, J.C.B., Lin, D.N.C., 1993, *ApJ* 409, 739  
 Korycansky, D. G., Pringle, J. E., 1995, *MNRAS* 272, 618  
 Latter, H. N., Ogilvie, G. I., 2006, *Icarus*, in press  
 Lightman, A. P., Eardley, D. M., 1974, *ApJ* 187, L1  
 Loska, Z., 1986, *Acta Astron.* 36, 43  
 Lubow, S. H., Ogilvie, G. I., 1998, *ApJ* 504, 983  
 Lubow, S. H., Pringle, J. E., 1993, *ApJ* 409, 360  
 Lyubarskij, Y. E., Postnov, K. A., Prokhorov, M. E., 1994, *MNRAS* 266, 583  
 Ogilvie, G. I., 1998, *MNRAS* 297, 291  
 Ogilvie, G. I., 2001, *MNRAS* 325, 231  
 Ogilvie, G. I., 2003, *MNRAS* 340, 969  
 Ogilvie, G. I., Lubow, S. H., 1999, *ApJ* 515, 767  
 Okazaki, A. T., 1985, *PASJ* 43, 75  
 Okazaki, A. T., Kato, S., 1985, *PASJ* 37, 683  
 Papaloizou, J. C. B., Lin, D. N. C., 1988, *ApJ* 331, 838  
 Papaloizou, J. C. B., Stanley, G. Q. G., 1986, *MNRAS* 220, 593  
 Schmit, U., Tscharnuter, W. M., 1999, *Icarus* 138, 173

## APPENDIX A: VERTICAL STRUCTURE OF THE DISC

Dimensional analysis of the equations of vertical structure leads us to introduce characteristic units  $U$  for the variables  $H$ ,  $\rho$ ,  $p$ ,  $T$  and  $F$  according to

$$U_H^{6+X-2Y} = \alpha R^{4-Y} \left( \frac{3C_\kappa}{16\sigma} \right) \Sigma^{2+X} 4A^2 \Omega^{-1} \Omega_z^{-6+2Y}, \quad (\text{A1})$$

$$U_\rho = \Sigma U_H^{-1}, \quad (\text{A2})$$

$$U_p = \Omega_z^2 U_H^2 U_\rho, \quad (\text{A3})$$

$$U_T = R^{-1} \Omega_z^2 U_H^2, \quad (\text{A4})$$

$$U_F = \alpha 4A^2 \Omega^{-1} U_H U_p. \quad (\text{A5})$$

Then let  $z = z_* U_H$ ,  $H = H_* U_H$ ,  $\rho(z) = \rho_*(z_*) U_\rho$ , etc., where starred quantities are dimensionless and satisfy the equations

$$\frac{dp_*}{dz_*} = -\rho_* z_*, \quad (\text{A6})$$

$$\frac{dF_*}{dz_*} = p_*, \quad (\text{A7})$$

$$\frac{dT_*}{dz_*} = -\rho_*^{1+X} T_*^{-3+Y} F_*, \quad (\text{A8})$$

$$p_* = \rho_* T_*, \quad (\text{A9})$$

$$\int_{-H_*}^{H_*} \rho_* dz_* = 1, \quad (\text{A10})$$

together with the boundary conditions  $\rho_*(\pm H_*) = T_*(\pm H_*) = 0$ . For reasonable values of  $X$  and  $Y$ , this problem has a unique solution that can be obtained numerically, with  $H_*$  determined as an eigenvalue.

Near the upper surface, the limiting behaviour is of the form  $F_* \rightarrow \text{constant}$ ,  $T_* \propto (H_* - z_*)$ ,  $\rho_* \propto (H_* - z_*)^{(3-Y)/(1+X)}$ ,  $p_* \propto (H_* - z_*)^{(4+X-Y)/(1+X)}$ .

The vertically averaged kinematic viscosity  $\bar{\nu}$  is given by

$$\bar{\nu} \Sigma = \int_{-H}^H \mu dz = \frac{\alpha U_p U_H}{\Omega} \int_{-H_*}^{H_*} p_* dz_*, \quad (\text{A11})$$

and therefore

$$\bar{\nu} \Sigma \propto \Sigma^{(10+3X-2Y)/(6+X-2Y)}. \quad (\text{A12})$$

## APPENDIX B: LONG-WAVELENGTH LIMIT

We consider the limit  $k \rightarrow 0$  of equations (25)–(29). One possible scaling is

$$s = k^2 s_2 + O(k^4), \quad (\text{B1})$$

$$u'_x = k u'_{x1} + O(k^3), \quad (\text{B2})$$

$$u'_y = k u'_{y1} + O(k^3), \quad (\text{B3})$$

$$u'_z = k^2 u'_{z2} + O(k^4), \quad (\text{B4})$$

$$\rho' = \rho'_0 + O(k^2), \quad (\text{B5})$$

$$p' = p'_0 + O(k^2), \quad (\text{B6})$$

which yields

$$-2\Omega \rho u'_{y1} = -i p'_0 + \partial_z (\mu \partial_z u'_{x1}), \quad (\text{B7})$$

$$2(\Omega - A) \rho u'_{x1} = -2i A \mu'_0 + \partial_z (\mu \partial_z u'_{y1}), \quad (\text{B8})$$

$$0 = \rho'_0 g_z - \partial_z p'_0, \quad (\text{B9})$$

$$s_2 \rho'_0 + u'_{z2} \partial_z \rho + \rho (i u'_{x1} + \partial_z u'_{z2}) = 0, \quad (\text{B10})$$

$$0 = (\gamma - 1) (4A^2 \mu'_0 - \partial_z F'_{z0}). \quad (\text{B11})$$

Therefore

$$s_2 \int_{-H}^H \rho'_0 dz = -i \int_{-H}^H \rho u'_{x1} dz, \quad (\text{B12})$$

$$2(\Omega - A) \int_{-H}^H \rho u'_{x1} dz = -2i A \int_{-H}^H \mu'_0 dz. \quad (\text{B13})$$

Since the hydrostatic and thermal balances are maintained in the perturbed equations to leading order,

$$\int_{-H}^H \mu'_0 dz = \frac{\partial(\bar{\nu}\Sigma)}{\partial\Sigma} \Sigma'_0, \quad (\text{B14})$$

and so

$$s_2 \Sigma'_0 = - \left( \frac{A}{\Omega - A} \right) \frac{\partial(\bar{\nu}\Sigma)}{\partial\Sigma} \Sigma'_0. \quad (\text{B15})$$

The dispersion relation for this mode is therefore

$$s = - \frac{4\Omega A}{\Omega_r^2} \frac{\partial(\bar{\nu}\Sigma)}{\partial\Sigma} k^2 + O(k^4). \quad (\text{B16})$$

Another possible scaling is

$$s = s_0 + k^2 s_2 + O(k^4), \quad (\text{B17})$$

$$u'_x = u'_{x0} + k^2 u'_{x2} + O(k^4), \quad (\text{B18})$$

$$u'_y = u'_{y0} + k^2 u'_{y2} + O(k^4), \quad (\text{B19})$$

$$u'_z = k u'_{z1} + O(k^3), \quad (\text{B20})$$

$$\rho' = k \rho'_1 + O(k^3), \quad (\text{B21})$$

$$p' = k p'_1 + O(k^3). \quad (\text{B22})$$

The horizontal components of the equation of motion at leading order yield

$$\rho(s_0 u'_{x0} - 2\Omega u'_{y0}) = \partial_z(\mu \partial_z u'_{x0}), \quad (\text{B23})$$

$$\rho[s_0 u'_{y0} + 2(\Omega - A) u'_{x0}] = \partial_z(\mu \partial_z u'_{y0}). \quad (\text{B24})$$

If  $u'_{x0}$ ,  $u'_{y0}$  depend on  $z$ , we obtain viscously damped epicyclic motions at this order. The modes satisfy a Sturm–Liouville equation and only one mode is undamped at leading order, being independent of  $z$ . For this solution, the right-hand sides vanish and

$$s_0^2 + 4\Omega(\Omega - A) = 0. \quad (\text{B25})$$

Therefore  $s_0 = \pm i\Omega_r$ ,  $u'_{x0} = U$  (independent of  $z$ ) and  $u'_{y0} = V = (s_0/2\Omega)U$ . The remaining equations at leading order yield

$$\begin{aligned} \rho s_0 u'_{z1} &= \rho'_1 g_z - \partial_z p'_1 \\ &+ \partial_z [2\mu \partial_z u'_{z1} + (\mu_b - \frac{2}{3}\mu)(iU + \partial_z u'_{z1})], \end{aligned} \quad (\text{B26})$$

$$s_0 \rho'_1 + u'_{z1} \partial_z \rho + \rho(iU + \partial_z u'_{z1}) = 0, \quad (\text{B27})$$

$$\begin{aligned} s_0 p'_1 + u'_{z1} \partial_z p + \gamma p(iU + \partial_z u'_{z1}) \\ = (\gamma - 1)(4A^2 \mu'_1 - 4A\mu iV - \partial_z F'_{z1}), \end{aligned} \quad (\text{B28})$$

$$\begin{aligned} F'_{z1} &= - \frac{16\sigma T^3}{3\kappa\rho} \left\{ \partial_z T'_1 \right. \\ &+ \left[ -(1+X) \frac{\rho'_1}{\rho} + (3-Y) \frac{T'_1}{T} \right] \partial_z T \Big\}, \end{aligned} \quad (\text{B29})$$

$$\frac{T'_1}{T} = \frac{p'_1}{p} - \frac{\rho'_1}{\rho}. \quad (\text{B30})$$

$$\mu'_1 = \frac{\alpha p'_1}{\rho}. \quad (\text{B31})$$

These can be solved, in principle, for  $u'_{z1}$ ,  $\rho'_1$ ,  $p'_1$ ,  $T'_1$ ,  $F'_{z1}$  (see below). Then the horizontal components of the equation of motion at order  $k^2$  yield

$$\begin{aligned} \rho(s_2 U + s_0 u'_{x2} - 2\Omega u'_{y2}) &= -i p'_1 \\ &+ i [2\mu iU + (\mu_b - \frac{2}{3}\mu)(iU + \partial_z u'_{z1})] \\ &+ \partial_z [\mu(iu'_{z1} + \partial_z u'_{x2})], \end{aligned} \quad (\text{B32})$$

$$\begin{aligned} \rho[s_2 V + s_0 u'_{y2} + 2(\Omega - A) u'_{x2}] &= -2iA\mu'_1 - \mu V \\ &+ \partial_z(\mu \partial_z u'_{y2}). \end{aligned} \quad (\text{B33})$$

We eliminate  $u'_{x2}$  and  $u'_{y2}$ , obtaining the solvability condition for these equations, by taking  $s_0$  times equation (B32) plus  $2\Omega$  times equation (B33), then integrating vertically:

$$\begin{aligned} 2\Sigma s_0 s_2 U &= \int_{-H}^H \left\{ s_0 [-ip'_1 - (\mu_b + \frac{7}{3}\mu)U \right. \\ &+ (\mu_b - \frac{2}{3}\mu)i\partial_z u'_{z1}] - 4\Omega A i\mu'_1 \Big\} dz. \end{aligned} \quad (\text{B34})$$

Note the contribution to this equation from the vertical motion, which also changes the relation between  $p'_1$  and  $U$ .

Under convenient assumptions ( $R$ ,  $\gamma$ ,  $\alpha$ ,  $\alpha_b$  being independent of  $z$ ) we have the analytical solution (cf. Ogilvie 2001)

$$u'_{z1} = s_0 W z, \quad (\text{B35})$$

$$\rho'_1 = -W z \partial_z \rho + A_\rho \rho, \quad (\text{B36})$$

$$p'_1 = -W z \partial_z p + A_p p, \quad (\text{B37})$$

$$T'_1 = -W z \partial_z T + A_T T, \quad (\text{B38})$$

$$F'_{z1} = -W z \partial_z F_z + A_F F_z. \quad (\text{B39})$$

In this solution, the Lagrangian perturbations of all quantities are proportional to the unperturbed quantities, meaning that the disc undergoes a kind of homogeneous (but dynamical) expansion. We find

$$\begin{aligned} s_0^2 W &= \Omega_z^2 (-2W - A_\rho + A_p) - (\alpha_b + \frac{4}{3}\alpha) \Omega_z^2 W (s_0/\Omega) \\ &- i(\alpha_b - \frac{2}{3}\alpha) \Omega_z^2 (U/\Omega), \end{aligned} \quad (\text{B40})$$

$$s_0 A_\rho = -iU - s_0 W, \quad (\text{B41})$$

$$\begin{aligned} s_0 A_p + \gamma(iU + s_0 W) \\ = (\gamma - 1) [4A^2(\alpha/\Omega)(A_p + W - A_F) \\ - 4A(\alpha/\Omega)iV], \end{aligned} \quad (\text{B42})$$

$$A_F = -(1+X)A_\rho + (4-Y)(A_p - A_\rho) - W. \quad (\text{B43})$$

We solve for  $W$ , then return to find  $s_2$  using

$$\int_{-H}^H p'_1 dz = (W + A_p)P, \quad P = \int_{-H}^H p dz. \quad (\text{B44})$$

Therefore

$$\begin{aligned} 2(\Sigma/P)s_2 U &= -i \left( 1 + \frac{4A\alpha}{s_0} \right) (W + A_p) \\ &- (\alpha_b + \frac{7}{3}\alpha)(U/\Omega) + (\alpha_b - \frac{2}{3}\alpha)i(s_0/\Omega)W. \end{aligned} \quad (\text{B45})$$

From the above equations  $s_2$  can be determined algebraically.